CALIBRATION OF A WIDE-ANGLE DIGITAL CAMERA SYSTEM FOR NEAR REAL TIME SCENARIOS

F. Kurz[a]*, R. Müller[a] , M. Stephani[b], P. Reinartz[a], M. Schroeder[a]

a German Aerospace Center (DLR), Remote Sensing Technology Institute, PO Box 1116, D-82230 Weßling, Germany
b Technische Universität München, Photogrammetry and Remote Sensing, Arcisstr. 21, D-80290 München, Germany
franz.kurz@dlr.de

Commission I, WG I/4

KEY WORDS: Aerial cameras, image series, near real time processing, direct georeferencing

ABSTRACT:
Near real time monitoring of natural disasters, mass events, and large traffic disasters with airborne SAR and optical sensors will be the focus of several projects in research and development at the German Aerospace Center (DLR) in the next years. For these projects, new airborne camera systems are applied and tested. An important part of the sensor suite plays the recently developed optical wide angle 3K camera system (3K = "3Kopf"), which consists of three non-metric off-the-shelf cameras (Canon EOS 1Ds Mark II, 16 MPixel). The cameras are aligned in an array with one camera looking in nadir direction and two in oblique sideward direction, which leads to an increased FOV of max 110°/ 31° in across track/flight direction. With this camera configuration, a high resolution, colour and wide-area monitoring task even at low flight altitudes, e.g. below the clouds, becomes feasible. The camera system is coupled to a GPS/IMU navigation system, which enables the direct georeferencing of the 3K optical images. The ability to acquire image sequences with up to 3Hz broadens the spectrum of possible applications in particular for traffic monitoring. In this paper, we present the concept of calibration and georeferencing which is adjusted to the requirements of a near real time monitoring task. The concept is based on straight forward georeferencing, using the GPS/IMU data to automatically estimate the not-measured boresight angles. To achieve this without measuring of ground control points (GCPs), we estimate on-the-fly boresight angles based on automatically matched 3-ray tie points in combination with GPS/IMU measurements. A prerequisite for obtaining robust results for the boresight angles is that the air plane attitude changes slightly during image taking; through these singular solutions can be avoided. Additionally, we assume known and fixed parameters of interior orientation. The determination of the interior orientation is performed ground based using a bundle adjustment of images from a calibration test field. The determination of the parameters of the interior orientation is repeated to check for their systematic changes in time. The proposed georeferencing and calibration concept was tested with images acquired during three flight campaigns in 2006. To evaluate the accuracy obtained by direct georeferencing using the proposed estimation procedure for the boresight angles without GCPs, the data are compared with the results of a bundle adjustment using GCPs and the GPS/IMU information. Summarizing, the RMSE of direct georeferencing with/without GCPs is *1.0m / 5.1m* in position and *0.5m / 1.0m* in height, at image scales of *1:20.000*. The accuracy without GCPs is regarded as acceptable for near real time applications. Additionally, it is shown that the parameter of the interior orientation remain stable during three repetitive calibrations on a test field for all three cameras.

1. INTRODUCTION

Airborne imaging sensors like digital cameras and SAR-systems become of increasing importance for near real time monitoring of extreme events in heavily populated areas. These events can be natural disasters like the Elbe flood in April 2006, mass events like the pope visit in Cologne in summer 2005 or traffic congestions after disastrous accidents. Airborne image data can contribute to an area wide situation overview.
For the management of such situations the data have to be directly transmitted to a situation awareness center where they can be utilized for decisions on "how to react".
In this paper a digital off-the-shelf camera system is tested for this purpose. This camera system was selected because it allows image sequences of up to 3Hz, which is very essential for traffic monitoring to determine vehicle velocities.
For operational use of the image data automatic georeferencing with knowledge of exterior and interior orientation is necessary. To accomplish the georeferencing in near real time only the camera calibration parameters and the recorded GPS/INS navigation data have to be used. Therefore, a method was developed for georeferencing which avoids the utilisation of GCPs. The main part of this method is the determination of the boresight misalignment angles only with tie points.
The investigations of this paper are part of an overall DLR project to develop a near real time airborne situation monitoring system with data transmission to a situation information center.
The paper is structured as follows. The DLR 3K-camera system is described in chapter 2. The image georeferencing concept for near real time applications is topic of chapter 3 and the 3K-camera calibration is described in chapter 4. Results and conclusions follow in chapter 5 and 6.

2. THE DLR 3K-CAMERA SYSTEM

DLR operates an optical sensor suite for experimental and operational flight campaigns. An important part of the sensor suite plays the recently developed optical wide angle 3K camera system (3K = "3Kopf"), which consists of three non-metric off-the-shelf cameras (Canon EOS 1Ds Mark II, 16 MPix). The cameras are arranged in a mount with one camera looking in nadir direction and two in oblique sideward direction (Fig 1), which leads to an increased FOV of max *110°/ 31°* in across track/flight direction. With this camera configuration, a high resolution, colour and wide-area monitoring task even at low flight altitudes, e.g. below the

clouds, becomes feasible. The camera system is coupled to a GPS/IMU navigation system, which enables the direct georeferencing of the 3K optical images.

Fig 1. DLR 3K-camera system consisting of three Canon EOS 1Ds Mark II, integrated in a ZEISS aerial camera mount

The Canon EOS 1Ds Mark II camera is the flagship model of the Canon EOS line and captures up to *32* consecutive frames with an image size of *4992x3328* pixels using a full frame CMOS sensor (*24x36mm*). The highest tested repetition rate for image acquisitions was 3Hz.

As a limitation for contiguous monitoring at this high repetition rates the internal buffer size of *165 MB* was identified, i.e. the camera must pause some seconds during flight campaigns to write the data from the internal buffer to the SD memory cards. If the repetition rate is below *0.5 Hz*, contiguous capturing is possible.

Thus, for the planning of flight campaigns with this camera the internal buffer size and the file sizes must be taken into account. The lossless compressed file size for images in the highest resolution is *15 MB*, which can be reduced using e.g. JPEG compression grade *10*, *8*, or *6* to *12*, *9*, or *4* Mbytes respective.

The onboard data link to a PC, which is required for near real processing of images, could be achieved based on a firewire connection with a data rate of *1.5 frames/s*. Further, an online connection to the navigation system is required for near real time processing based on GPS/IMU measurements.

Fig 2 illustrated the image acquisition geometry of the DLR 3K-camera system. Based on the use of *50 mm* Canon lenses, the relation between airplane flight height, ground coverage, and pixel size is shown, e.g. the pixel size at a flight height of *1000 m* above ground is *15 cm* and the image array covers up *2.8km* in width.

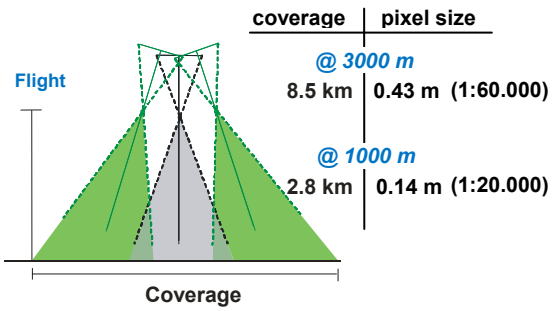

Fig 2. Illustration of the image acquisition geometry. The tilt angle of the sideward looking cameras is approx. 35°.

3. NEAR REAL TIME GEOREFERENCING OF IMAGE SEQUENCES

The basis for all direct georeferencing formulas is the collinearity concept, where the coordinates of an object point $\mathbf{r}^m$ expressed in any earth bound mapping coordinate frame are related to image coordinates $\mathbf{r}^{Camera}$ derived from the measured pixel position in the sensor's coordinate frame. The rigorous relationship between 2D image coordinates and 3D object coordinates is given by

$$\mathbf{r}^m = \mathbf{r}^m_{Camera} + s \cdot \mathbf{R}^m_{Body} \cdot \mathbf{R}^{Body}_{Camera} \cdot \mathbf{r}^{Camera} \quad (1)$$

where boresight missalignement matrix $\mathbf{R}^{Body}_{Camera}$ denotes the rotation from the camera to the body coordinate frame (IMU coordinate frame), which has to be calibrated, and $\mathbf{R}^m_{Body}$ denotes the rotation around the angles from the body to a mapping coordinate frame, which is derived from the angular measurements. The position of the camera projection centre

$$\mathbf{r}^m_{Camera} = \mathbf{r}^m_{GPS} - \mathbf{R}^m_{Body}\mathbf{r}^{Body}_{GPS} + \mathbf{R}^m_{Body}\mathbf{r}^{Body}_{Camera} \quad (2)$$

is calculated from the measured position $\mathbf{r}^m_{GPS}$ reduced by the pre-mission measured lever arms $\mathbf{r}^{Body}_{GPS}$ from the body frame origin to the measured position and $\mathbf{r}^{Body}_{Camera}$ from the body frame origin to the sensor projection centre, both expressed in the body coordinate frame. The lever arms are taken into account within the post-processing of the GPS/IMU data. For single imagery the scale factor s is determined by the intersection of the sensor pointing direction with a given DEM also expressed in the mapping coordinate frame. It is noted that the DEM transformation into the mapping frame should at least include a resampling to the image resolution or better.

The interior orientation is described by mapping column(i)/row(j) values to the sensor coordinate frame with the focal length c by

$\mathbb{N}^2 \rightarrow \mathbb{R}^3$:

$$i, j \rightarrow \mathbf{r}^{Camera} = (x_{i,j} - x_0, y_{i,j} - y_0, -c)^T \quad (3)$$

for frame cameras.

For small acquisition areas an UTM can be used as mapping coordinate frame. In this case the measured heading angle has to be corrected for the meridian convergence. The attitude observations for each image are therefore modelled as

$$\mathbf{R}^m_{Camera}(t) \equiv \mathbf{R}^{UTM}_{Camera} = \mathbf{R}^{UTM}_{IMU}(r, p, y) \cdot \mathbf{R}^{IMU}_{Camera}(r_b, p_b, y_b) \quad (4)$$

where r, p, y are the measured roll, pitch, and yaw and r_b, p_b, y_b the corresponding boresight angles.

The determination of the interior orientation is described in chapter 4.1 and the procedure to calculate the boresight angles is described in chapter 4.2.

4. CALIBRATION OF DLR 3K–CAMERA SYSTEM

4.1 Determination of interior orientation

Bundle adjustment is considered the most appropriate tool to calculate 3D-object coordinates from multiple image coordinate measurements. In a least square adjustment process the image coordinates and control point coordinates are considered as the "observations", while the exterior orientation (position and attitude) of the images and the object coordinates of homologues points constitute the "unknowns". In some well defined cases, beside the exterior orientation, also the interior orientation parameters of the

camera are considered as "further unknowns" (resp. not precisely enough known in advance). This procedure is well known as "self calibrating block adjustment".
The role of control points in such an adjustment process is twice: On the first hand they allow for the calculation of the whole block position and attitude (block datum) and on the second hand they help to eliminate systematic errors e.g. introduced either from the image coordinate system or systematic errors of the environment, e.g. atmospheric refraction.
Using an adequate calibration field with some well defined object points with known coordinates and a set of special arranged images of it, the task of self calibrating block adjustment could be turned into the determination of the interior orientation of the camera, mainly.
In order to obtain precise and reliable interior orientation parameters subpixel image measurements are desirable and the redundancy of the adjustment should be as high as possible.
As the exterior orientation in our set up is delivered by GPS/IMU measurements only, the absence of control points asks for a precise and reliable interior orientation parameters of the cameras in advance in order to avoid systematic effects in point determination.
In case of available control points in a real scenario they could be used to evaluate the obtained accuracy of object points (check points).
Bundle adjustment with ground control points (GCPs) allows also integrating the GPS/IMU measurements as "observations" of the unknowns of image exterior orientation. Systematic components of this observations, due to incorrect reduction e.g. of the GPS-antenna to the centre of projection of the central perspective of the images may result.
Using all three CANON EOS cameras, two calibration sets of image data of our calibration field where acquired on 11.05.2006 and on the 30.05.2006. The impact of lens changing for the Nadir Camera was simulated and studied, also. Five parameters of interior orientation were estimated, the focal length c_I, the principal point $x_{0,I}$ and $y_{0,I}$, and two radial distortion parameters A_1 and A_2. The radial distortion Δr is then calculated by

$$\Delta r = A_1\left(r^3 - r\cdot r_0^2\right) + A_2\left(r^5 - r\cdot r_0^4\right) \qquad (5)$$

where r is the distance to the frame center and r_0 the reference radius.
Image measurement was mainly based on point matching using triplets; from there *1/5-1/10* of an image pixel of *7.2µ* could be achieved. More calibration results are given at *5.2* (Table 1).

4.2 Determination of boresight misalignment

4.2.1 Concept of boresight estimation using 3 ray tie points

The determination of boresight misalignment for aerial cameras is usually based on a bundle adjustment using tie points, ground control points (GCPs) and GPS/IMU data. The solution of these bundle adjustment equations for the determination of the unknown boresight misalignment will be singular, if no GCPs are introduced, as the images could rotate freely.
Fast in-situ determination of boresight misalignment could be required in near real time scenarios, as the look directions of the cameras may have changed due to new adjustments or camera replacements. The use of GCPs in bundle adjustments usually involves manual interaction and is therefore not applicable for near real time applications, whereas tie points can be determined automatically by matching.
In this context, the difference between 2ray tie points and 3ray tie points gets important, as for 2ray tie points bundle adjustment converge for every common image rotation set and for 3ray tie points only for the "correct" image rotations.
The property of an exemplary 3ray tie point is illustrated in Fig 3, where the image attitude based on the GPS/IMU measurements without regarding the boresight misalignment is displayed in red. At the correct image attitude (black) including the boresight misalignment, an exemplary 3ray tie point converges to a point. This behaviour is illustrated in Fig 3 for the three attitude angles roll, pitch, and yaw, where the movement of the airplane is illustrated with blue arrows.

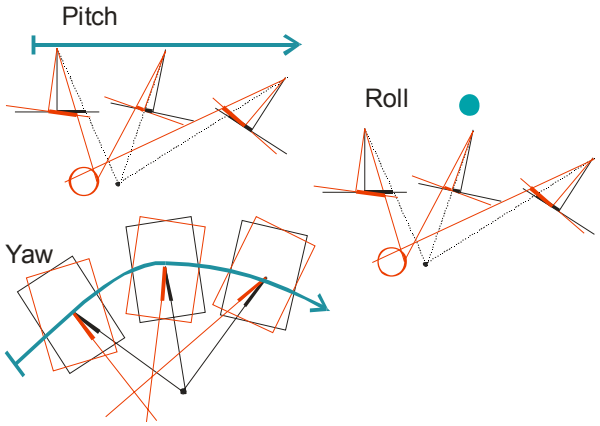

Fig 3 Illustration of 3ray tie points for images without regarding boresight misalignment (red circles) and for images with the correct boresight angles (black dots)

This property of 3ray tie points could be exploited in a bundle adjustment to determine the boresight misalignment without using GCP. Most important condition for this approach is that image attitude angles must change measurable between the three acquisitions. In other words, if there is no change in the image attitudes roll, pitch, and yaw, all 3ray tie points converge for every boresight angle and the bundle adjustment will be singular. Thus, the degree of attitude change greatly influences the accuracies of estimated boresight angles. Here, not an overall range of change, but the minimum $\Delta\alpha$ of all incremental changes of attitudes for consecutive images is most decisive.

$$\Delta\alpha = \min\left(|r_1 - r_2|, |r_2 - r_3|, |p_1 - p_2|, |p_3 - p_2|, |y_1 - y_2|, |y_3 - y_2|\right) \qquad (6)$$

Fig 4 is the result of a simulation which shows exemplarily the relation between the minimal incremental change and the theoretical standard deviation of the three boresight angles for a nadir looking Canon EOS camera. This simulation reveals that the accuracy is increasing with increasing change of attitudes $\Delta\alpha$, and that the determination of the boresight roll angle turns out to be less accurate than the other boresight angles.

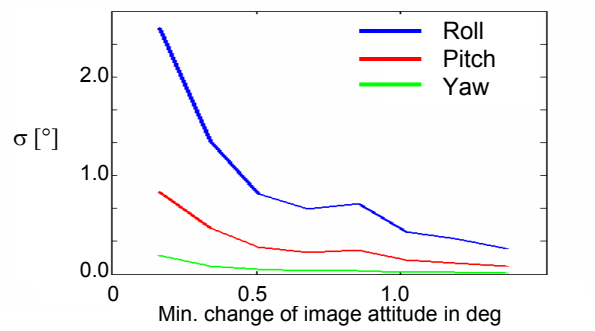

Fig 4 Relation between attitude change and boresight angle accuracy

4.2.2 Estimation of boresight misalignment with a bundle adjustment using only 3ray tie points

For the estimation of boresight misalignment, a bundle adjustment using the GPS/IMU measurements and automatically matched 3ray tie points is conceived. Additional tie points between left/right looking images and the nadir images are introduced to stabilize the relative camera orientations (Fig 5). In case of 3K-camera system, altogether nine boresight angles, three for each camera, must be estimated. Due to the tilted cameras, boresight angles up to *35°* are possible, which impede commonly used approximations for boresight misalignment.

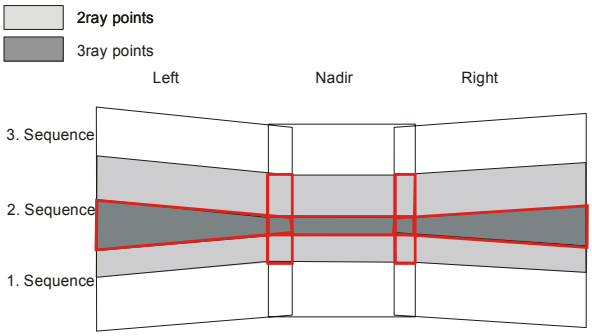

Fig 5 Proposed matching scheme (red zones): matched 3ray tie points in three consecutive left, nadir, and right looking images as well as 2ray tie points between left/right and nadir images.

The functional model for one observed 3ray tie point with the unknown object coordinates $(X_T,\ Y_T,\ Z_T)$ and the camera position $(X_0,\ Y_0,\ Z_0)$ is described using equation (1) in equation (7).

$$\begin{bmatrix} x_{i,I} - x_{0,I} \\ y_{i,I} - y_{0,I} \\ -c_I \end{bmatrix} = \left(s \cdot \mathbf{R}^{UTM}_{Camera-I}\right)^{-1} * \begin{bmatrix} X_T - X_0 \\ Y_T - Y_0 \\ Z_T - Z_0 \end{bmatrix} \tag{7}$$

where $x_{i,I}$ and $y_{i,I}$ are measured tie points for images $i = [1,2,3]$ and camera $I \in \{L, N, R\}$.

The rotation matrix is calculated using the measured IMU attitudes and the unknown boresight angles according equation (4). The transformation (7) by applying the collinearity condition leads to the final equation of measured 3ray tie points

$$x_{i,I} = x_{0,I} - c_I \frac{R_{1,1}(X_T - X_0) + R_{2,1}(Y_T - Y_0) + R_{3,1}(Z_T - Z_0)}{R_{1,3}(X_T - X_0) + R_{2,3}(Y_T - Y_0) + R_{3,3}(Z_T - Z_0)} \tag{8}$$

$$y_{i,I} = y_{0,I} - c_I \frac{R_{1,2}(X_T - X_0) + R_{2,2}(Y_T - Y_0) + R_{3,2}(Z_T - Z_0)}{R_{1,3}(X_T - X_0) + R_{2,3}(Y_T - Y_0) + R_{3,3}(Z_T - Z_0)} \tag{9}$$

where $R \equiv \left(R^{UTM}_{Camera-I}\right)^{-1}$.

A different functional model must be applied for 2ray tie points between left/right looking to the nadir looking camera, as the images are acquired almost from the same position and the estimation of object coordinates will therefore be close to singular. Hence, two collinearity equations are combined by elimination of the object coordinates, which is exemplarily shown for the second image sequence of nadir and left cameras in equation (10).

$$\begin{bmatrix} x_{2,L} - x_{0,L} \\ y_{2,L} - y_{0,L} \\ -c_L \end{bmatrix} = \left(s_L \mathbf{R}^{UTM}_{Camera-L}\right)^{-1} * s_N \mathbf{R}^{UTM}_{Camera-N} * \begin{bmatrix} x_{2,N} - x_{0,N} \\ y_{2,N} - y_{0,N} \\ -c_N \end{bmatrix} \tag{10}$$

Transforming (10) by elimination of the scale factors leads to the image coordinate equations

$$x_{2,L} = x_{0,L} - c_L \frac{R_{1,1}(x_{2,N} - x_{0,N}) + R_{2,1}(y_{2,N} - y_{0,N}) - R_{3,1}c_N}{R_{1,3}(x_{2,N} - x_{0,N}) + R_{2,3}(y_{2,N} - y_{0,N}) - R_{3,3}c_N} \tag{11}$$

$$y_{2,L} = y_{0,L} - c_L \frac{R_{1,2}(x_{2,N} - x_{0,N}) + R_{2,2}(y_{2,N} - y_{0,N}) - R_{3,2}c_N}{R_{1,3}(x_{2,N} - x_{0,N}) + R_{2,3}(y_{2,N} - y_{0,N}) - R_{3,3}c_N} \tag{12}$$

where $R \equiv \left(R^{UTM}_{Camera-L}\right)^{-1}\left(R^{UTM}_{Camera-N}\right)$.

For reasons of simplicity, the image coordinates from the nadir image $x_{2,N}$ and $y_{2,N}$ are introduced as constants into the bundle adjustment.

The nine unknown boresight angles together with the unknown object coordinates are finally estimated within a least-squares adjustment using a Gauss-Markov model according to the described functional model.

5. RESULTS

5.1 Results of interior orientation

Careful handling of the whole camera system is a prerequisite for maintaining the interior orientation elements stable over time. In our experiment the calibrated focal length by focussing the cameras ad infinitum was rather stable (v. Table 1). The two parameters of radial distortion generate radial image coordinate displacement values in the range of +50 to –200 microns resp. of 7 to 28 pixels. Obviously they have to be taken into account for precise object point determination. Due to the mechanical lay out of the bayonet attachment of lenses to the camera body the image coordinates of the principal points varies. Therefore lens changes should be reduced to a minimum. After a careful calibration the image acquisition system turns out to be precise and stable.

	Left side	Nadir 11.05.	Nadir 30.05.	Nadir* 30.05.	Right side.
Calib. Focal Length c [mm]	51.316	51.017 ±0.021	50.995 ±0.022	50.963 ±0.022	51.156
Principal point x_0 [mm]	+0.213	+0.083 ±0.004	+0.064 ±0.007	+0.052 ±0.006	-0.076
Principal point y_0 [mm]	-0.081	-0.031 ±0.006	-0.054 ±0.009	-0.099 ±0.008	+0.022
Radial Distortion A_1 [m^{-2}]	-57.539	-55.880 ±0.403	-57.290 ±0.785	-55.930 ±0.767	-56.673
Radial Distortion A_2 [m^{-4}]	29568.7	28337.9 ±1654.2	30265.5 ±1613.8	28396.5 ±1654.0	28210.5
Redundancy	11507	1307	584	467	3699
Sigma Naught σ_0 [µ]	0.76	0.82	1.34	1.36	1.00

*After Lens Change

Table 1 Results of camera calibration

5.2 Results of boresight misalignment

5.2.1 Database

Images from two flight campaigns, *27.07.2006* and *02.09.2006*, were used for the estimation of boresight misalignment. On *27.07.*, images of DLR area in Oberpfaffenhofen were acquired from *1000m* above ground, which results in a ground pixel size of *15cm* in nadir direction (*data I*). Later on *02.09.*, images of the motorway *A8* south of Munich were acquired from *2000m* above ground (*data IIa*) and again images from DLR area in Oberpfaffenhofen (*data IIb*) during the same flight. Additionally, GPS/IMU measurements and data from a GPS reference station were processed to obtain camera positions and image attitudes. For DLR area in Oberpfaffenhofen, a dense net of GCP is available.

Data	Δα>0.1°	Δα>0.2°	Δα>0.5°
I	34%	19%	4%
IIa	7%	1%	0%
IIb	30%	1%	0%

Table 2 Fraction of overlapping sequences with the attitude change Δα useable for boresight determination.

Table 2 shows the fraction of sequences with a minimal attitude change Δα during three consecutive images resp. all three consecutive images in overlap. Due to windy conditions at data take I, the fraction of image sequences with minimal attitude change are higher than at data take IIa and IIb. One conclusion is that for every data take there are sufficient image sequences, which could be used for boresight determination without using GCPs.

5.2.2 Determination of boresight angles

The goal was to determine the boresight misalignment and also to detect changes in the period July till September 2006, even if the sensor platform was not modified during this time. The boresight angles were estimated in three ways, first by applying a bundle adjustment with blocks of up to 20 images using GCPs (1), then same as before including the GPS positions (2), and last the proposed bundle adjustment without using GCPs (3). Last method was applied on various image sequences selected with the criteria Δα>0.2°.

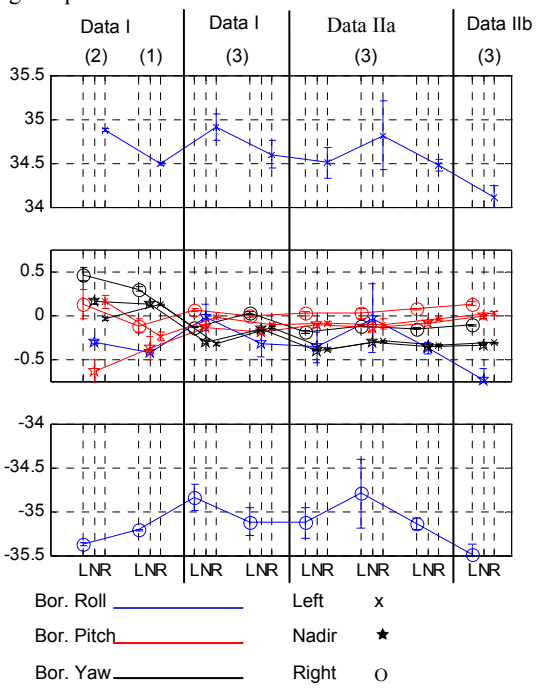

Fig 6 Results of boresight estimation by bundle adjustment with or without using GCP for data I, IIa, and IIb. The standard deviation is indicated.

Fig 6 shows that the results of the bundle adjustment with GCPs differ from the results without using GCPs. The low flight height at data take *I* at *1000m* was problematic, as there were not enough GCPs covered up by the images, which may lead to the small bias in the boresight yaw and pitch angles. In the rest of the data sets, all yaw and pitch angles remain constant for all cameras, whereas the boresight roll angle shows higher variations. In general, for all methods, the boresight roll angle is weakly defined. This is caused by the small basis (s. Fig 3 right) in flight direction for method (3) and due to the elongated image blocks when using (1) or (2). Another conclusion is that a significant change of boresight angles could not be determined with the proposed methods, as the accuracies are not high enough. At this point a suitable test procedure as proposed by Bäumker could be taken into account.

5.3 Accuracies of direct georeferencing

The accuracies of the direct geocoding process described before were evaluated based on data take I (Table 3). For this, the images were ortho-projected to an already existing DEM using the estimated image orientations from (1) and (3). The positions of check points were used to calculate the RMSE. Heights were calculated first through forward intersection and then compared with DEM heights to calculate RMSE.

	$RMSE_{XY}$	$RMSE_Z$	Σ points
(1)	*1.03m*	*0.48m*	*21*
(3)	*5.11m*	*3.51m*	*21*

Table 3 Accuracies of geocoded images

6. CONCLUSIONS

We described the calibration of the new DLR 3K-camera system separated in the ground calibration of interior orientations and in the boresight angle determination. The ground calibration was performed with a self calibrating block adjustment based on images from a calibration test field. Repetitive calibration showed sufficient high long term stability of the interior parameters of Canon EOS cameras.
A new approach for boresight angle determination using only 3ray tie points and GPS/IMU measurements was proposed. The results were validated during two flight campaigns and compared to results of a bundle adjustment using GCPs and GPS/IMU measurements. Advantage of this approach is that the boresight determination could be performed on-flight, e.g. to check the recent exterior orientation to coarse changes or after modifications of the 3K-camera geometry. Nevertheless, the obtained accuracies depend mainly on the attitude changes occurring during the flight mission.

7. LITERATURE

Skaloud, J., Schaer, P., 2003. *Towards a more rigorous boresight calibration.* In: Proceedings ISPRS International Workshop on Theory, Technology, and Realities of Inertial / GPS Sensor Orientation. Spain, 22.09.-23.09.2003

Jacobsen, K., *Calibration aspects in direct georeferencing of frame imagery*, In: Int. Archives PhRS (34), 1 I, pp. 82-89, Denver 2002.

Bäumker, M., Heimes F.-J., 2001. *New Calibration and Computing Method for Direct Georeferencing of Image and Scanner Data Using the Position and Angular Data of an Hybrid Inertial Navigation System.* In: Proceedings OEEPE Workshop Integrated Sensor Orientation, Hannover, 17.-18.9.2001

Bäumker, M. 2007. *Kalibration und Umrechnung von INS- und potogrammetrischen Winkeln für beliebige gegenseitige Anordnung*. In: Proceedings of the 14. Internationalen geodätischen Woche, Obergurgl 2007, 11.02.-17.02.2007. Österreich.

Redweik, P., Jacobsen, L.&K., 2007. *Handling uncalibrated GPS/IMU data for medium scale mapping*, PFG (2), 99-110

Reinartz, P., Lachaise, M., Schmeer, E., Krauss, T., Runge, H., 2006. *Traffic monitoring with serial images from airborne cameras*, ISPRS Journal of Photogrammetry & Remote Sensing 61 (2006), 149-158.